Catalysis Today 426 (2024) 114388

Contents lists available at ScienceDirect

Catalysis Today

journal homepage: www.elsevier.com/locate/cattod

Sisal-derived acid-char molybdenum catalyst for reductive deoxygenation of sulfoxides

Tiago A. Fernandes [a,*], Tiago A.G. Duarte [b,1], Ana S. Mestre [b], Maria J.G. Ferreira [a], Ana M. Botelho do Rego [c], Ana M. Ferraria [c], Marina V. Kirillova [a], Ana P. Carvalho [b,*], Maria José Calhorda [d]

[a] Centro de Química Estrutural, Institute of Molecular Sciencies, Associação do Instituto Superior Técnico para a Investigação e Desenvolvimento, Universidade de Lisboa, 1049-001 Lisboa, Portugal
[b] Centro de Química Estrutural, Institute of Molecular Sciencies, Departamento de Química e Bioquímica, Faculdade de Ciências, Universidade de Lisboa, 1749-016 Lisboa, Portugal
[c] BSIRG-iBB-Institute for Bioengineering and Biosciences and Associate Laboratory i4HB—Institute for Health and Bioeconomy, Dep. de Engenharia Química, Instituto Superior Técnico, Universidade de Lisboa, Av. Rovisco Pais, 1049-001 Lisboa, Portugal
[d] BioISI— Instituto de Biossistemas e Ciências Integrativas, Departamento de Química e Bioquímica, Faculdade de Ciências, Universidade de Lisboa, Campo Grande, Lisboa 1749-016, Portugal

ARTICLE INFO

Keywords:
Sisal
Acid-mediated carbonization
Molybdenum complexes
Immobilized heterogeneous catalysts
Deoxygenation
Sulfoxide reduction

ABSTRACT

The deoxygenation of sulfoxides is a rather important reaction from both synthetic and biological points of view, due to the potential of sulfides as intermediates in a variety of processes. Homogenous Mo-based catalysts successfully perform the reduction of diphenyl sulfoxide to diphenyl sulfide with high yields but present the well-known limitations regarding recovery and recycling. Thus, in the present work, two new supported catalysts were prepared through the immobilization of molybdenum precursor species (dichlorodioxodi(aquo)molybdenum(VI) and sodium molybdate), onto a sisal-derived acid-char (S13.5), obtained from rope industry wastes by acid-mediated carbonization. The heterogeneous Mo-based materials were characterized by IR spectroscopy, elemental analysis, ICP, solid state NMR, XPS, and SEM, and were evaluated as catalysts for the reduction of sulfoxides to sulfides in the presence of phenylsilane as reducing agent under different reaction conditions. The influence of various experimental parameters, including reducing agent type and amount, solvent type, and acid promoter were investigated. Catalytic studies revealed that both catalysts deoxygenate sulfoxides at 120 °C in toluene solution with high yields (up to 97%). The MoO_2Cl_2 derived catalyst shown to be highly efficient in the reduction of diaryl, alkylaryl, dibenzyl, and dialkyl sulfoxides to the corresponding sulfoxides using phenylsilane as reductant and no need of acid promoter.

1. Introduction

The development of effective ways to recover and recycle homogenous catalysts is essential from an economic, environmental, and long-term perspective, since most of these catalysts are expensive and, in many cases, harmful to the environment. A well-known technique to overcome the drawbacks of homogeneous catalysts is their immobilization on a solid support, allowing a simple isolation from the reaction medium and consequently their re-use for consecutive cycles [1–4]. This strategy allows lower investment and improved resource saving. The support for the catalyst should be wisely chosen, and the use of by-products, or even wastes, from other industries leads to an overall more sustainable process aligned with the principles of circular economy. On the other hand, the use of renewable raw materials as feedstocks fulfills the goals of green chemistry. Among other solids, a great number of carbon materials, such as activated carbons, carbon nanotubes, and structured mesoporous carbons, share these characteristics as they can be produced from renewable precursors and/or wastes and have been successfully tested as supports for homogeneous catalysts [5–11]. Activated carbons have a relevant nanoporous network, but

* Corresponding authors.
E-mail addresses: tiago.a.fernandes@tecnico.ulisboa.pt (T.A. Fernandes), ana.carvalho@fc.ul.pt (A.P. Carvalho).
[1] Current affiliation: Chemistry Department and CQ-VR, University of Trás-os-Montes e Alto Douro, 5001–801 Vila Real, Portugal.

https://doi.org/10.1016/j.cattod.2023.114388
Received 21 March 2023; Received in revised form 31 July 2023; Accepted 15 September 2023
Available online 17 September 2023
0920-5861/

their surface chemical composition inhibits direct catalyst immobilization, requiring thus, in most cases, multi-step preparation processes. Conversely, chars (also known as biochars when prepared from biomass) obtained by conventional or innovative carbonization routes usually present an incipient nanopore structure associated with a high content of heteroatoms on surface functional groups [12]. The conventional carbonization (also referred as pyrolysis) of residues with high carbon content, given their complex heteropolysaccharides containing galacturonic acid, arabinose, galactose, etc., as is the case of agro-industrial wastes, yield electron donor functional groups, namely oxygen functional groups, such as carboxyl, phenolic, and lactones, which effectively bind transition metals [13,14]. Hydrothermal carbonization has attracted great attention since it provides carbon materials - hydrochars - with high oxygen content and slightly acid surface chemistry [12,15] via a more sustainable process (i.e. water as a solvent, low temperatures, and autogenous pressure). Acid-chars obtained by acid-mediated carbonization (AMC) are promising carbon materials which so far have been tested mainly for adsorption processes [12,16–22], and scarcely employed for catalytic applications [20,23]. It must be noted that AMC allows to control the density of the acid-char, which may attain very high values, along with a very rich acidic surface chemistry [16,17]. The possibility of using a high-density support to immobilize a homogeneous catalyst is quite important since the higher the density, the easier the separation of the solid after the reaction. Also, the variety of precursors used to prepare acid-chars includes liquid and solid feedstocks with a high moisture content that inhibits their valorization through conventional routes [12,21]. Another important property of acid-chars is their acidic surface chemistry that makes them particularly interesting to be used as support for complexes via direct immobilization [23]. In fact, for most carbon materials, the acid surface groups needed to interact with the complex are commonly introduced through post-synthesis methods, which are not needed in the case of AMC. Recently the acid-chars obtained by H_3PO_4-mediated carbonization of cauliflower leaves were considered as promising materials for the removal of Cu(II) and Pb(II) from aqueous medium due to the presence of hydroxyl and carboxyl functionalities that favor their coordination to the metals [22].

Due to the high amount of polysaccharides, sisal proved to be a suitable resource to prepare acid-chars [16,17] and so it was the starting material chosen to prepare the supports of the present study. Sisal is the strongest vegetal fiber that has been used for centuries for rope manufacture and is still primarily used in our days as a natural raw material for the rope industry [24]. Being derived from the leaves of *Agave sisalana*, an autochthone plant from Mexico that also grows in tropical countries in Africa, West Indies, and Far East [24], sisal belongs to the group of hard fibers that includes flax, abaca, jute, coir, among others [25]. In 2014, global production of sisal fiber reached 261,235 tons, Brazil being the largest producing country according to the 2018 FAOSTAT data (2020 report) [26]. The residues generated during the rope manufacturing process are commonly recycled to produce low-quality ropes or used as fuel [27].

Considering all that was mentioned above, in this study we have followed a three steps approach to synthesize the molybdenum heterogeneous catalysts using sisal rope residues as the starting material of the support (Fig. 1).

Since the goal was to prepare catalysts for reduction of sulfoxides to sulfides, choosing a molybdenum-based catalyst was an obvious option. In fact, in nature, there are several molybdenum-based enzymes that can perform sulfoxides deoxygenation, such as methionine sulfoxide, or biotin sulfoxide reductases [28,29]. The deoxygenation of sulfoxides is a rather important reaction from both synthetical and biological points of view, due to the potential use of sulfides as intermediates in a variety of transformations. This reaction is crucial in biology to prevent cells damage, while it can also produce chiral auxiliaries for the synthesis of biologically active compounds [30]. High valent dioxomolybdenum(VI) complexes are known for their ability to catalyze oxygen-transfer reactions of sulfides, phosphines, and olefins. The MoO_2Cl_2/silane system is very efficient towards the hydrosilylation of aldehydes and ketones, to the corresponding silyl ethers, for the reduction of imines, amides, esters, sulfoxides, and pyridine *N*-oxides to the corresponding amines, alcohols, sulfides, and pyridines [31]. Other Mo-based catalytic systems can act as efficient homogeneous catalysts for the reduction of diphenyl sulfoxide to diphenyl sulfide and could be extended to diaryl, alkylaryl, dibenzyl, and dialkyl sulfoxides with excellent product yields [32].

The present study reports the catalytic reduction of various sulfoxides to sulfides in the presence of two Mo-catalysts immobilized onto sisal-derived acid-char, in line with the increasing interest to develop new methods of deoxygenation [33–36] through more sustainable catalytic processes.

2. Experimental

Sodium molybdate, diphenyl, methyl phenyl, dibenzyl, dibuthyl and methyl sulphoxides, phenylsilane and ethylsilane were obtained from Sigma-Aldrich, with purities > 99%, and were used as received. A diethyl ether solution of $[MoO_2Cl_2(H_2O)_2]$ was synthesized from an aqueous solution of sodium molybdate in concentrated HCl, as described in the literature (see detailed description in SI) [37]. The solvents and all commercial products were used without further purification. Residues of sisal were provided by a rope industry (Cordex, Portugal) and used as starting material. The synthesis of the acid-chars required H_2SO_4 (Sigma-Aldrich, 95–98%).

2.1. Acid-char synthesis

The acid-char was obtained by acid digestion and carbonization of sisal residues [16,17,23]. Briefly, 40 mL of a 13.5 M solution of H_2SO_4 and 4.0 mg of sisal, previously cut into pieces smaller than 0.4 cm, were mixed. The mixture was heated at 55 °C and kept stirring for 15 min. A dark liquor obtained after filtration was heated for 6 h at 90 °C using a thermostatic water bath (VWR Scientific Model 1201). The acid-char was collected by filtration, washed with distilled water until neutral pH, dried overnight at 100 °C (Heraeus Instruments). After drying, a black and hard solid was obtained with 38% yield. Finally, the solid was crushed in an agata mortar to recover a fine powder (particles with dimensions < 0.297 mm) that is designated as S13.5. Elemental analysis (%): found C 60.5, H 4.2, S 0.5, N 0.2. FTIR (KBr/cm^{-1}): 3448 (br), 2922 (w), 2852 (w), 1708 (vs), 1614 (vs), 1171 (m), 1023 (m), 799 (w).

2.2. Catalysts immobilization

Two different molybdenum functionalized acid-chars were synthesized. MoCl@S13.5 was obtained using dichlorodioxodi(aquo)molybdenum(VI), $[MoO_2Cl_2(H_2O)_2]$, as molybdenum source, and MoO@S13.5 using sodium molybdate ($Na_2MoO_4{\cdot}2H_2O$).

To prepare the MoCl@S13.5 catalyst, 250 mg of S13.5, 75 mg

Fig. 1. Summary of steps for catalyst manufacturing: from sisal rope production waste to immobilized Mo complexes catalyst.

(0.32 mmol, 9.4 wt% (Mo)) of $[MoO_2Cl_2(H_2O)_2]$ and 20 mL of dry CH_2Cl_2 were mixed and allowed to react at 40 °C under vigorous stirring and nitrogen atmosphere for 18 h. The obtained supported catalyst was washed with CH_2Cl_2 (3 × 15 mL) and dried to dryness on a vacuum line at room temperature. A dark blue powder - heterogeneous catalyst MoCl@S13.5 - was obtained with 98% yield. Elemental analysis (%): found C 48.7, H 3.2, S 0.5. ICP-OES Analysis for Mo: 8.0%. FTIR (KBr/cm^{-1}): 3428 (br), 1713 (vs), 1614 (s), 1029 (w), 953 (m), 914 (m).

MoO@S13.5 was synthesized following the same experimental conditions but using $Na_2MoO_4{\cdot}2\,H_2O$ (92 mg, 0.45 mmol, 13.1 wt% (Mo)) as molybdenum source. At the end a dark brown powder was obtained with 94% yield. Elemental analysis (%): found C 51.2, H 3.5, S 0.5. ICP-OES Analysis for Mo: 3.3%. FTIR (KBr/cm^{-1}): 3447 (br), 1708 (vs), 1614 (vs), 943 (w), 881 (m), 817 (m).

2.3. Catalytic assays

The catalytic reactions of diphenyl sulfoxide reduction were carried out in a Radleys Carousel 12 Plus Reaction Station, a thermostated glass parallel reaction station, operating at ambient atmosphere and under vigorous stirring at 120 °C and using 3 mL of toluene as solvent (up to 5 mL total volume). In a typical experiment, substrate (0.25 mmol) and catalyst (20 mg) were introduced in the toluene acidified solution (0.005 mM HCl), followed by the addition of phenylsilane (0.25 mmol). Some parameters were changed to investigate the effects of catalyst loading, temperature, solvent, reductant, acid promoter, and substrate (for the exact reaction conditions see captions of figures and tables).

For the reuse/regeneration assays, the catalyst was initially tested using 5 mmol of diphenyl sulfoxide, 30 mg of catalyst, 3 mL of toluene, and 1 eq. of phenylsilane. After that, the recovered material was either reused as it was or after washing with dichloromethane, followed by filtration, and drying at 120 °C for 1 h. Reuse tests were conducted in the same experimental conditions.

2.4. Characterization and instrumentation

Elemental analysis (EA) was carried out by the Microanalytical Service Microanalyses of the University of Vigo. CHN analyses were performed on a Fisons EA 1108; Mo quantification was performed by ICP-OES on a Perkin Elmer Optima 4300DV using Yttrium as internal standard (fresh catalysts) and on a Perkin Elmer Optical Emission Spectrometer Optima 2000 DV LAIST, Laboratory of Analyses, IST (recovered catalyst). Infrared spectra (FTIR, 4000–400 cm^{-1}) were recorded on a Nicolet 6700 instrument in KBr pellets using 2 cm^{-1} resolution (abbreviations: vs – very strong, s – strong, m – medium, w – weak, br – broad, sh – shoulder).

For solid-state nuclear magnetic resonance (ss-NMR) analysis, samples S13.5, MoCl@S13.5 and MoO@S13.5 (~200 mg) were packed into 7 mm O.D. rotors equipped with Kel-F caps. ^{13}C Cross Polarization/Magic Angle Spinning (CP/MAS) spectra were obtained at 75.49 MHz on a Bruker/Tecmag Wide Bore NMR, with spinning rates of circa 3 kHz and at least 900 scans. The Hartmann–Hahn condition was optimized using glycine, also the external reference to set the chemical shift scale (^{13}CO at 176.1 ppm). Whenever necessary, ^{13}C CP/MAS spectra were obtained with suppression of the spinning side bands, achieved by using the TOSS (Total suppression of Spinning Sidebands) sequence [38]. In these experiments, contact times of 3 ms, 90° RF pulses of 4 μs and relaxation delays of 5 s were used.

X-ray photoelectron spectroscopy (XPS) analyses were performed using a Kratos XSAM800. Samples were irradiated with the Al Kα radiation (hν=1486.6 eV). Experimental conditions and details about data treatment were the same as described elsewhere [39]. Charge accumulation effects were corrected setting the binding energy (BE) position of the first peak fitted to C 1 s regions (assigned to graphitic carbon) to 284.6 eV. Sensitivity factors here used were: C 1 s:0.278; O 1 s:0.78; N 1 s:0.42; Mo 3d:3.21; Cl 2p:0.891.

Scanning electron microscopy coupled with energy dispersive X-ray spectroscopy (SEM-EDS) analysis was carried out with a microscopy Hitachi, S-2400 instrument with an accelerating voltage set to 15 kV and various amplifications. All the samples were coated with palladium previously to measurements.

The determination of the acid-char pH at the point of zero charge (pH_{PZC}) was obtained using a Symphony SP70P pH meter. The pH_{PZC} was performed by a reverse mass titration method according with literature [40,41] (see page 3 of SI for experimental details). The surface chemistry characterization of the materials was complemented by evaluating the amount of the total surface acidic groups according to the methodology described in ref. 42. Briefly, 20 mL of 0.1 M NaCl solution was added to 150 mg of carbon material and stirred for 72 h, the resulting suspension was filtered, and the final solution were titrated to an endpoint of pH 7 with 0.01 M NaOH. The total number of acid sites corresponds to the amount of NaOH consumed in the acid-base titration.

The apparent density and moisture of the acid-char were determined according with the procedure previously described in the literature for powdered materials [17] (see description of the methodology in page 3, SI).

The reaction progress was monitored by withdrawing small aliquots of the reaction mixture after different periods of contact time. The samples were analyzed by GC using cyclooctane as internal standard. In the case of diphenyl sulfoxide reduction, the analyses were made in a Shimadzu QP2100-Plus GC/MS system and a capillary column (Teknokroma TRB-5MS/TRB-1MS) operating in the linear velocity mode (Fig. S1). The analyses of the reaction media corresponding to the reduction of other substrates (methyl phenyl sulfoxide, dibenzyl sulfoxide, dibutyl sulfoxide and dimethyl sulfoxide) were performed in an Agilent Technologies 7820 A series gas chromatograph (He as carrier gas) equipped with the FID detector and the BP5/SGE (30 m × 0.22 mm × 0.25 μm). In any case, GC peak assignment was made by comparison with chromatograms of standard samples.

3. Results and discussion

3.1. Acid-char functionalized materials

The acid-char derived from sisal, S13.5, was selected as support for molybdenum catalysts immobilization due to its functionalized acidic surface, as demonstrated by the pH_{PZC} value of 1.8. In line with this value, the total amount of acid surface groups was estimated as 4.23 mmol H^+/g_{carbon}. The acid-char presented a moisture content of 8.7% and its apparent density (tapped), after dried, was 688 kg/m^3.

The S13.5 acid-char was used as support matrix for two oxomolybdenum compounds, $[MoO_2Cl_2(H_2O)_2]$ and $Na_2MoO_4{\cdot}2H_2O$. The immobilized catalysts were fully characterized by FTIR, SEM, ss-NMR, EA, ICP-OES, and XPS.

Fig. 2 shows the FTIR spectra of the acid-char, the homogenous Mo catalysts ($[MoO_2Cl_2(H_2O)_2]$ and $Na_2MoO_4{\cdot}2H_2O$), and the functionalized materials (MoCl@S13.5 and MoO@S13.5).

The FTIR spectrum corresponding to the S13.5 acid-char presents the same profile as those reported in literature for this material [16,17,23]. Besides the vibrations corresponding to oxygen surface functionalities (i.e., -OH, C═O, C−O, C−O−C) it is important to highlight the vibrations attributed to the sulfonic acid group (-SO_3H) which appear as a strong broad band centered around 1143 cm^{-1} and a smaller one at around 1022 cm^{-1} [17,43,44].

The free complex, $[MoO_2Cl_2(H_2O)_2]$, exhibits one strong band at 1614 cm^{-1} which is assigned to the bending vibration of δ(HOH). The bands at 960 and 920 cm^{-1} are assigned, respectively, to the antisymmetric and symmetric stretching vibrations of ν(Mo═O). The band at 766 cm^{-1} could arise from the vibrational mode ν(Mo−O−Mo) indicating the presence of bridging or polymeric species in the molybdenum precursor,[45], and the band at 569 cm^{-1} can be assigned to ν(Mo−OH_2) [46]. The bridging units may be formed when isolating the

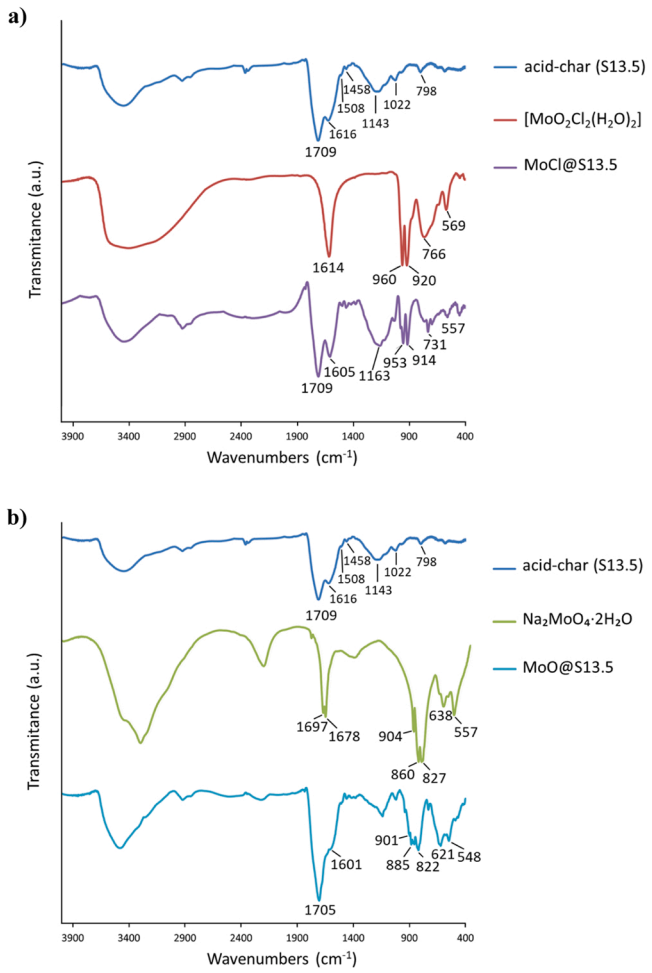

Fig. 2. FTIR analysis of a) acid-char, $[MoO_2Cl_2(H_2O)_2]$, and MoCl@S13.5; b) acid-char, $Na_2MoO_4{\cdot}2\,H_2O$, and MoO@S13.5.

solid by drying up the ether solution.

MoCl@S13.5 exhibits the characteristic bands from the Mo complex, namely the strong band at 1605 cm^{-1}, assigned to the bending vibration of δ(HOH). The narrow bands at 953 and 914 cm^{-1}, slightly shifted to smaller wavenumbers, can still be assigned to the stretching vibration of ν(Mo═O). The bands assigned to vibration of ν(Mo−O−Mo) and ν(Mo−OH_2), are shifted towards 731 cm^{-1} and 557 cm^{-1}, respectively.

The major peaks for free molybdate ($Na_2MoO_4{\cdot}2H_2O$) are assigned to the Mo═O group, and appear at 904, 860, and 827 cm^{-1}. The two strong bands at 1697 and 1678 cm^{-1} are assigned to the bending vibration of δ(HOH) and the band at 557 cm^{-1} to ν(Mo−OH_2).

In the spectrum of MoO@S13.5 the bending vibrations of δ(HOH) are hidden by bands characteristic of the acid-char. The observed strong bands at 901, 885, and 822 cm^{-1} are assigned to the ν(Mo═O) vibration which confirms that the Mo atom is tetrahedrally coordinated to oxygen atoms.

For all the samples, the broad absorption bands centered around 3400 cm^{-1} and 1600 cm^{-1} are assigned, respectively, to the stretching and deformation modes of hydroxyl groups of adsorbed water. The bands at ~2920 cm^{-1} and ~2850 cm^{-1} are due to ν(C-H) modes, and evidence the presence of aliphatic moieties from the acid-char matrix. The strong band at 1709 cm^{-1} observed in the char and in both immobilized catalysts spectra is assigned to ν(C═O) stretching vibrations, indicating the presence of ketones, esters, or aldehyde functional groups. The band at ~1616 cm^{-1} and the shoulder at ~1500 cm^{-1} are attributed to ν(C═C) stretching modes from aromatic moieties of the acid-char [17]. The broad peaks at ~1170 cm^{-1} (acid-char), 1163 cm^{-1} (MoCl@S13.5), and 1133 cm^{-1} (MoO@S13.5), besides the previous attribution to sulphonic groups, can also be due to the presence of the C−O stretching vibrations and O−H deformation vibrations of alcohols, phenols, ethers, or esters, usually observed between 1450 and 1000 cm^{-1} [18,47,48].

Summarizing, from the analysis of FTIR spectra it is possible to conclude that the functionalization of the surface of the acid-char with both Mo compounds was successfully achieved. Indeed, several functional groups with variable acidities and coordination sites on the acid-chars surface can interact with molybdenum species in diverse ways, resulting in a variety of Mo environments.

The morphology of the acid-char S13.5, and catalysts MoCl@S13.5 and MoO@S13.5 was characterized by SEM–EDS. The microphotographs of S13.5 (Fig. 3a and b) reveal the smooth and uniform surface characteristic of this acid-char [16,17]. The immobilization of both molybdenum compounds results in a significative change of the surface topology that becomes rougher, as can be observed in the images reproduced in Fig. 3c-f. The SEM-EDS of MoCl@S13.5 and MoO@S13.5 and the corresponding Mo and O distribution (Fig. 4) suggest a homogeneous dispersion of molybdenum species over the surface of the acid-char. The EDS analysis made for MoCl@S13.5 (Figs. 3g and h, 4b) confirms that, as expected, the main components of the motifs covering the surface of the acid-char are molybdenum and chlorine. The SEM-EDS studies on MoO@S13.5 also identifies the main elements of the Mo catalyst (molybdenum, oxygen, and sodium) covering the acid-char surface (Fig. S2).

The support and the immobilized catalysts were analyzed by solid-state NMR (Figs. 5, S3 and S4). The ^{13}C CP/MAS NMR spectrum of the acid-char S13.5 shows the presence of carbonyl groups (180–200 ppm), aromatic carbons (100–150 ppm), carbons that are linked to electronegative atoms such as O, N or S (60–80 ppm), as well as carbons present in alkyl chains (0–50 ppm), in line with the NMR spectrum recently published by the authors for this type of carbon material [16]. The comparison of the NMR spectrum of the acid-char S13.5, produced by H_2SO_4-mediated carbonization of sisal, with those of biochars obtained by slow or fast pyrolysis of biomass (i.e., corn stover or switchgrass heat treated at 500 °C under nitrogen flow) [49] clearly reveals the higher degree of heteroatom functionalization of the sisal derived acid-char with more intense peaks in the region of carbonyl groups, carboxyl or amide carbon, O/N/S-aryl carbon, and N-alkyl carbon.

Since the amount of molybdenum species immobilized in the surface of the acid-char is, in any case, quite small (8.0% for MoCl@S13.5 and 3.3% for MoO@S13.5), only small differences on the overall appearance of the ^{13}C CP/MAS NMR spectra are observed. In, fact a detailed analysis of the spectra of the acid-char and both catalysts immobilized reveals that the major differences are found in the alkyl region of the spectrum, where, as highlighted in Fig. 5, more intense and defined peaks are observed. This change is especially evident in the case of sample MoCl@S13.5 for which higher and sharper signals in the region of 60 ppm and around 10 ppm are observed. It is possible that oxygen and/or nitrogen atoms in the support interact with the metal and that changes the environment of the carbon atoms attached directly to these atoms, which translates into different chemical shifts in that area [50]. The presence of the metal complex may also alter the mobility of the aliphatic chains. The signals around 10 ppm are sharper which is consistent with higher mobility of these groups.

The two catalysts were studied by XPS to improve the chemical characterization. Detailed XPS regions for Mo 3d, Cl 2p, O 1 s and C 1 s (Fig. 6) and survey spectra (not shown) were acquired.

The Mo 3d region of the MoCl@S13.5 sample was fitted with a single doublet with a spin-orbit split of 3.2 eV with the main component, Mo $3d_{5/2}$ centred at 233.3 ± 0.1 eV assigned to Mo(VI) [51,52]. For the MoO@S13.5 sample 2 doublets were required. The lowest intensity one has its main component Mo $3d_{5/2}$ centred at 231.6 ± 0.1 eV and is assignable to Mo(V). The most intense doublet has its main component Mo $3d_{5/2}$ centred at 234.3 ± 0.1 eV which is higher than the usual

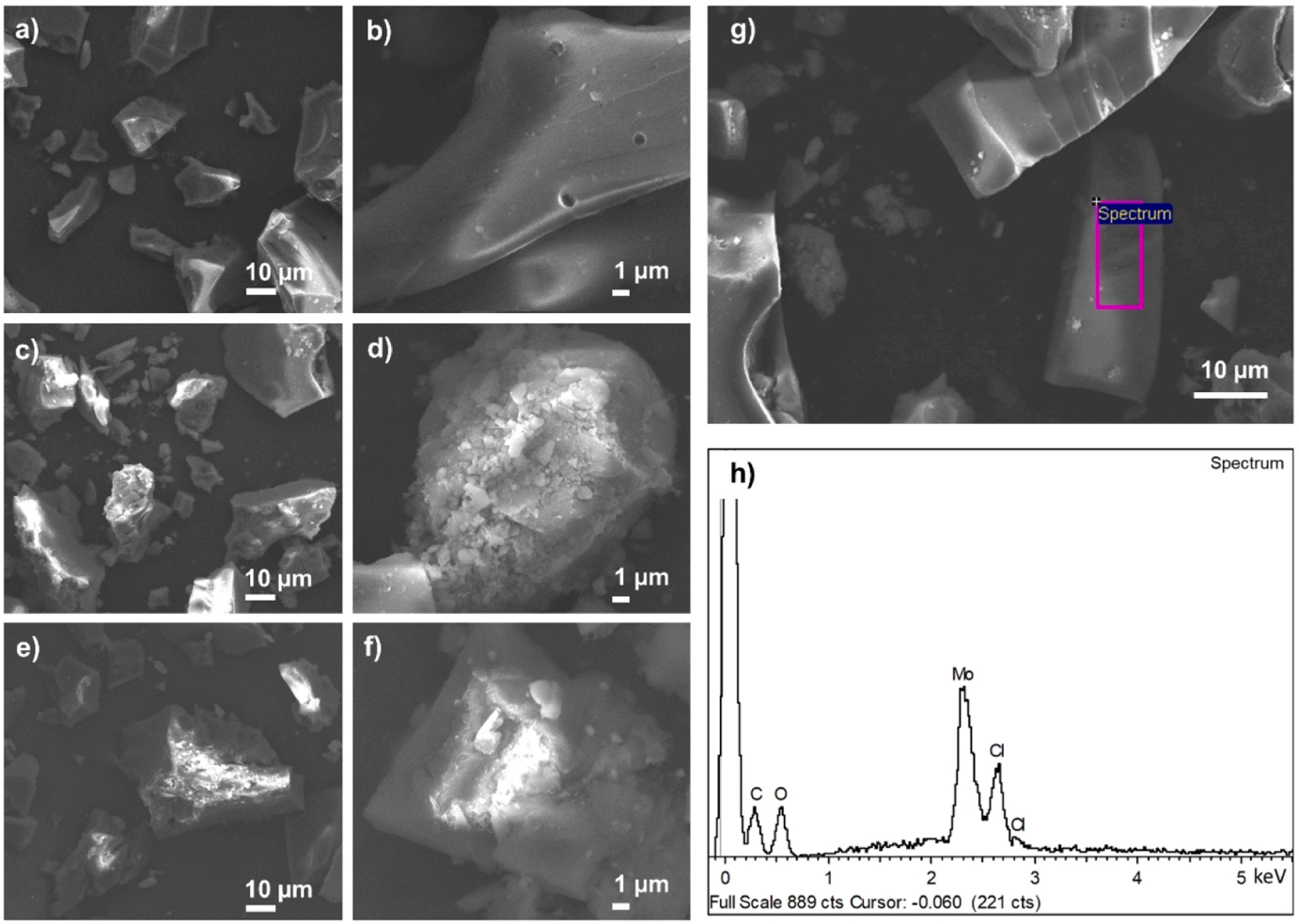

Fig. 3. SEM images of: a) and b) acid-char (S13.5); c) and d) MoCl@S13.5; e) and f) MoO@S13.5; g) selected area for EDS analysis of MoCl@S13.5; h) EDS spectrum of selected area. Images a), c), and e) were obtained at 500 × magnification; b), d), and f) at 3000 × magnification, and g) at 150 × magnification.

values in literature for Mo(VI). This result will be further discussed when analysing the O 1 s region.

Cl 2p was detected in both immobilized catalysts with one doublet for MoO@S13.5 (where no chlorine was expected) and two doublets for MoCl@S13.5. Both samples present the doublet with a spin-orbit split of 1.6 eV and the main component Cl $2p_{3/2}$ centred at 200.1 ± 0.1 eV, which is assigned to chlorine bonded to carbon [53] and is attributed to some retention of CH_2Cl_2. For MoCl@S13.5 a second doublet with Cl $2p_{3/2}$ centred at 198.5 ± 0.1 eV was needed, being assignable to chloride ion and attributed to unreacted precursor. Since the atomic ratio Cl^-/Mo is 0.12, it means that the most part of the detected Mo was modified. The atomic ratio Cl (in CH_2Cl_2)/C in MoCl@S13.5 and in MoO@S13.5 is, respectively, 0.007 and 0.005. Vestigial amounts, therefore.

The O 1 s region for both samples was fitted with 3 peaks centered at 531.5 ± 0.1 eV, 532.6 ± 0.1 eV, and 533.9 ± 0.1 eV. The first component may contain some contribution from a MoO_x oxygen [54], from inorganic hydroxyl groups but also (and mainly) from the oxygen doubly bonded to carbon in aromatic carbonyl and/or carboxylic groups. The second one is assignable to the same functional groups (carbonyl and carboxylic) but not bound to aromatic systems. The third one is assigned to oxygen singly bonded to carbon both in alcohols, ethers, carboxylic but especially typical of anhydrides (O═C–O–C═O) and organic carbonates [55]. However, for the sample MoO@S13.5, three extra components were needed to complete the fitting at 535.2 ± 0.1 eV, 537.3 ± 0.1 eV and 539.1 ± 0.1 eV. These binding energies are typical of oxygen in water molecules, respectively, isolated, moderately aggregated and strongly aggregated [55]. The presence of water molecules solvating the Mo(VI) ion could explain the high BE value found in the MoO@S13.5 sample. However, the existence of differential charge effects cannot be discarded [56,57].

Finally, for the C 1 s region, the binding energies and atomic percentages extracted from the fitted peaks presented in Fig. 6 are gathered in Table 1.

These results are consistent with the complex nature of the acid-char already demonstrated by ss-NMR and FTIR data.

3.2. Catalysis

Deoxygenation of sulfoxides catalyzed by molybdenum compounds usually proceeds in the presence of a small amount of acid promoter, which is needed to activate the catalyst and accelerate the reaction thus affecting both the total product yield and the initial reaction rate (W_0) [31], and a reducing agent to bind the oxygen released by the substrate. Therefore, the activity of the immobilized catalysts, MoCl@S13.5 and MoO@S13.5, was evaluated in the reduction of diphenyl sulfoxide to the corresponding sulfide, starting with the commonly used phenylsilane as reducing agent and a toluene acidified with 0.005 mM, HCl solution as solvent (Scheme 1). Further assays were then planned to optimize reaction conditions, such as, catalyst loading, others reducing agents, and solvents. The results obtained are collected in Table 2.

Blank tests demonstrated that in the absence of catalyst or phenylsilane no reaction occurred (Table 2, entries 1 and 2, respectively). The acid-char was also tested as catalyst leading to a yield of 6.1 % or less of

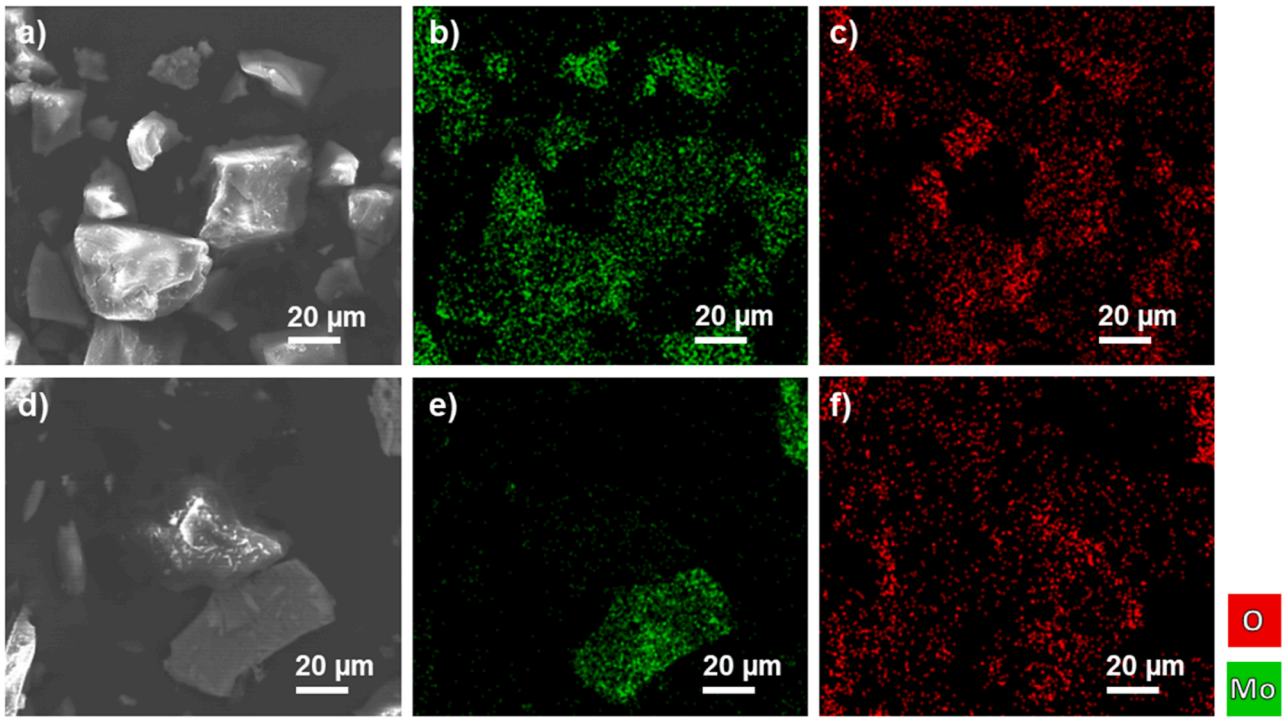

Fig. 4. Morphology characterization using SEM-EDS: SEM images of a) MoCl@S13.5 with an EDS analysis of Mo and O distribution (b and c). SEM images of d) MoO@S13.5 with an EDS analysis of Mo and O distribution (e and f).

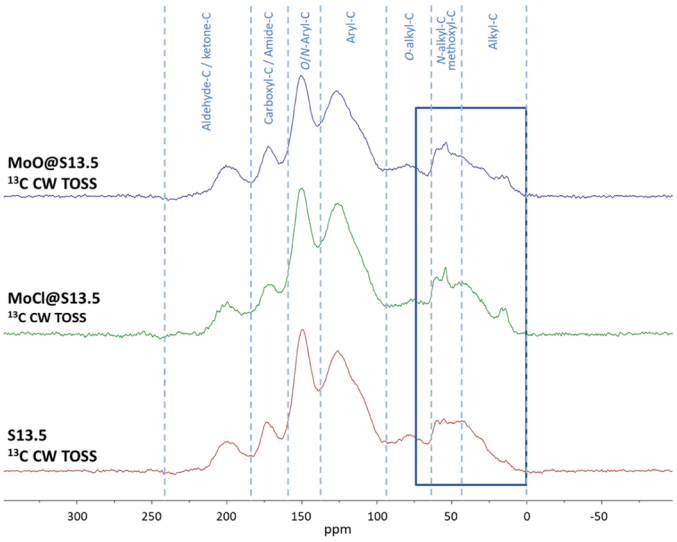

Fig. 5. Solid State ^{13}C CP/MAS TOSS (Total Suppression of Spinning Sidebands) spectra of the indicated samples.

diphenyl sulfide (Table 2, entries 11 and 12). The homogeneous catalyst was also tested under equivalent conditions, i.e., 5 mg of $[MoO_2Cl_2(H_2O)_2]$ (0.02 mmol Mo) attaining 100% yield after 2 h of reaction (Table 2, entry 13).

To select the most suitable solvent for the reaction using the immobilized catalysts, different solvents were tested, and product yield was determined after 22 h of reaction time. The results quoted in Table S1 show that, for a load of 20 mg of catalyst, higher sulfoxide yields were achieved in THF (90.5%) than in toluene (only 71.5%, see entries 4 and 6). However, it must be noted that the reflux temperature of toluene was crucial to avoid the formation of diphenyl sulfone as a by-product. In fact, for THF at 70 °C the 90.5% yield of diphenyl sulfide is associated with 6.4% of the by-product diphenyl sulfone (Table S1, entry 6) [58, 59]. Aiming at a potential application of more environmentally friendly solvents than toluene or tetrahydrofuran [60], the reduction of diphenyl sulfoxide in ethanol or isopropanol was also carried out (Table S1, entries 8 and 9, respectively). Most likely due to the low reflux temperature of these solvents the maximum yield achieved was 4.0%.

Once toluene was selected as the preferred solvent, the catalytic activities of the two Mo-based materials were studied under the same experimental conditions, demonstrating that MoCl@S13.5 stands out as the best performing catalyst (see for instance, Table 2, entries 5 and 8 or entries 6 and 9) in line with its higher Mo content (8.0 versus 3.3% for MoO@S13.5). Moreover, comparing, for example, the data of Table 2, entries 9 and 12, it is plausible to assume that part of the yield reached by MoO@S13.5 (12.4%) is partly due to the surface groups of the acid-char which by itself has a yield of 6.1%. For MoCl@S13.5 the same assumption can be made but, in this case, having less relevance for the global yield. Nevertheless, in an attempt to improve the yield of diphenyl sulfide, an additional assay with 20 mg of MoO@S13.5 was made and the amount of $PhSiH_3$ increased to 2 eq. The increase of the reaction yield was indeed observed (Table 2, entries 8 and 10) but the value was still lower than that obtained using MoCl@S13.5 and only 1 eq. of $PhSiH_3$ (30.9% versus 71.5%) was reached.

Considering the more favorable yields obtained with MoCl@S13.5 in the previously analyzed results, further experiments were performed using only this material. In the first set of assays, the effect of the MoCl@S13.5 loading (5, 10, 20, and 30 mg) was studied, as shown in Fig. 7, revealing that the higher catalyst loading leads to the higher conversion of diphenyl sulfoxide into diphenyl sulfide, and also initial reaction rate (W_0).

The effect of the reducing agent amount was evaluated for both MoCl@S13.5 (Schemes 2) and S13.5 support. As expected, higher conversion of diphenyl sulfoxide into diphenyl sulfide is observed when more equivalents of $PhSiH_3$ are added. As reported on Fig. 8, with a loading of 20 mg of MoCl@S13.5, not only higher yield but also a faster reaction (71.5% and 3.5 $\times 10^{-4}$ M s^{-1}, respectively) were observed with the addition of 1 eq. of phenylsilane (Fig. 8, violet line and Table 2, entry

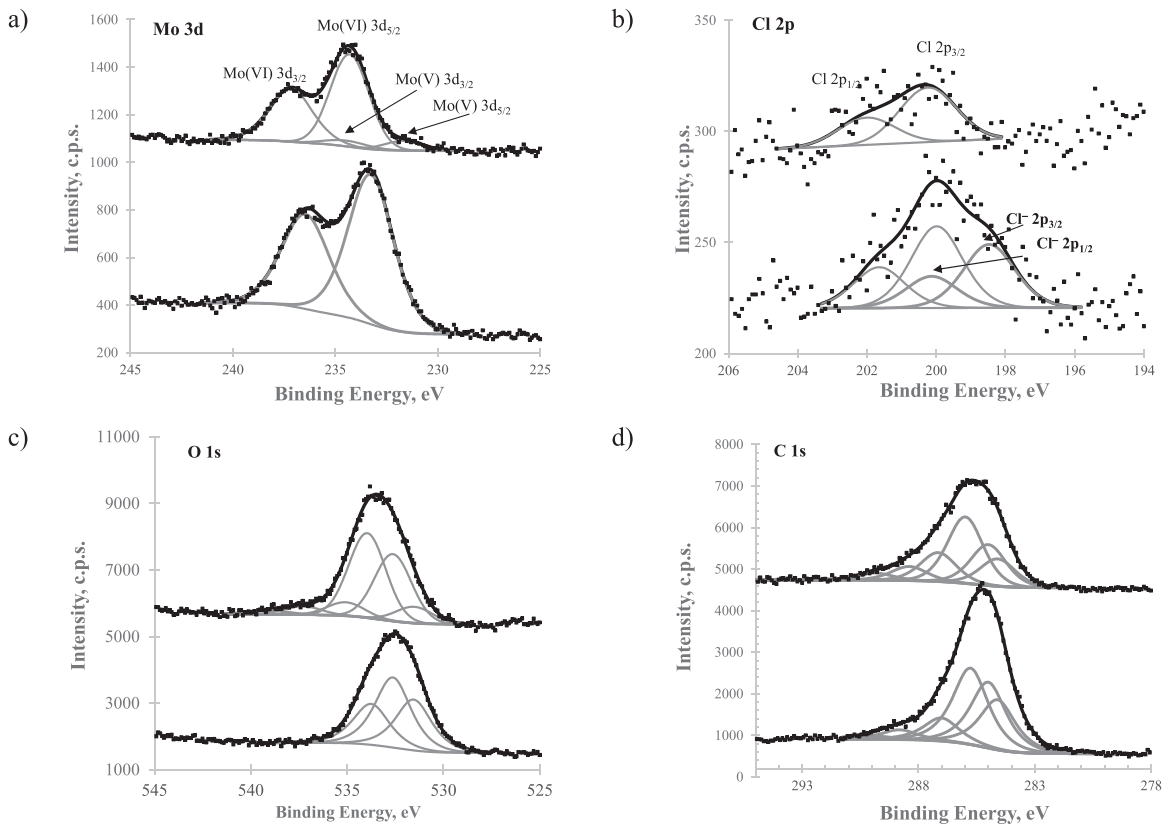

Fig. 6. XPS detailed regions a) Mo 3d, b) Cl 2p, c) O 1s, and d) C 1s obtained for MoCl@S13.5 (bottom) and MoO@S13.5 (top). Intensity values for MoO@S13.5 were added of a constant to set off spectra for clarity sake.

Table 1
XPS C 1 s region fitted with six components: binding energies, relative atomic percentage and assignments.

	MoCl@S13.5		MoO@S13.5		Assignments
	BE (± 0.1 eV)	At. %	BE (± 0.1 eV)	At. %	
C 1s 1	284.6	21.9	284.6	14.9	Aromatic **C**–**C**, **C**–H
C 1s 2	285.0	28.8	285.0	22.1	Aliphatic **C**–**C**, **C**–H
C 1s 3	285.8	33.5	286.0	36.0	**C**–O
C 1s 4	287.0	10.1	287.1	15.6	Aromatic C=O, epoxide
C 1s 5	288.8	4.2	288.4	7.6	Carboxylate
C 1s 6	289.9	1.4	289.9	3.8	Carboxylic, anhydride, organic carbonate

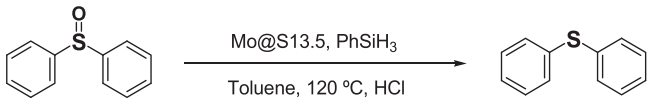

Scheme 1. -Schematic representation of diphenyl sulfoxide reduction under the conditions reported in Table 2.

5), than with 0.5 eq. (59.2%, and 2.0×10^{-4} M s^{-1}, respectively, Table S2, entry 4). The initial reaction rate dropped down at the same time (Fig. 8b).

These data demonstrate the important role of the $PhSiH_3$ amount to potentiate the intrinsic catalytic properties of the acid char that reaches 38.6% yield when using 30 mg and 2 eq. of reductant. This is not surprising since $PhSiH_3$ is consumed in the reaction ($PhSiH_3 + Ph_2SO \rightarrow PhSi(OH)H_2 + Ph_2S$).

Table 2
Diphenyl sulfoxide reduction into the corresponding sulfide in the presence of MoCl@S13.5 or MoO@S13.5 using phenylsilane as reducing agent in toluene.[a].

Entry	Cat. (loading mg)	$PhSiH_3$ (Substrate equivalents)	Yield[b] [%]
1	-	1	<1
2	MoCl@S13.5 (10)	0	<1
3	MoCl@S13.5 (5)	1	9.8
4	MoCl@S13.5 (10)	1	31.5
5	MoCl@S13.5 (20)	1	71.5
6	MoCl@S13.5 (30)	1	94.5
7	MoO@S13.5 (10)	1	10.3
8	MoO@S13.5 (20)	1	13.1
9	MoO@S13.5 (30)	1	12.4
10	MoO@S13.5 (20)	2	30.9
11	S13.5 (20)	1	4.9
12	S13.5 (30)	1	6.1
13	$[MoO_2Cl_2(H_2O)_2]$ (5)	1	100[c]

[a] Reaction conditions: catalyst (5, 10, 20 or 30 mg; 0.8, 1.65, 3.3, 5.0 mol% Mo, respectively), diphenyl sulfoxide (0.25 mmol), phenylsilane (0.25 or 0.50 mmol), acidified toluene solvent (0.005 mM, HCl, up to 3 mL of the total reaction volume), 120 °C, 22 h.
[b] Yield of sulfide product [(moles of product/moles of substrate) × 100 %].
[c] Yield after 2 h of reaction.

Ethylsilane was also tested as reducing agent, the results being presented in Table S3. In the presence of 1 eq. of reducing agent and 20 mg of MoCl@S13.5 much higher yields are obtained with $PhSiH_3$ (71.5% of diphenyl sulfide yield versus 6.9% for Et_3SiH; Table S3, entries 4 and 6, respectively). Even doubling the amount of Et_3SiH no relevant increase of the product yield is observed (6.9–11.1%, Table S3, entries 6 and 7, respectively).

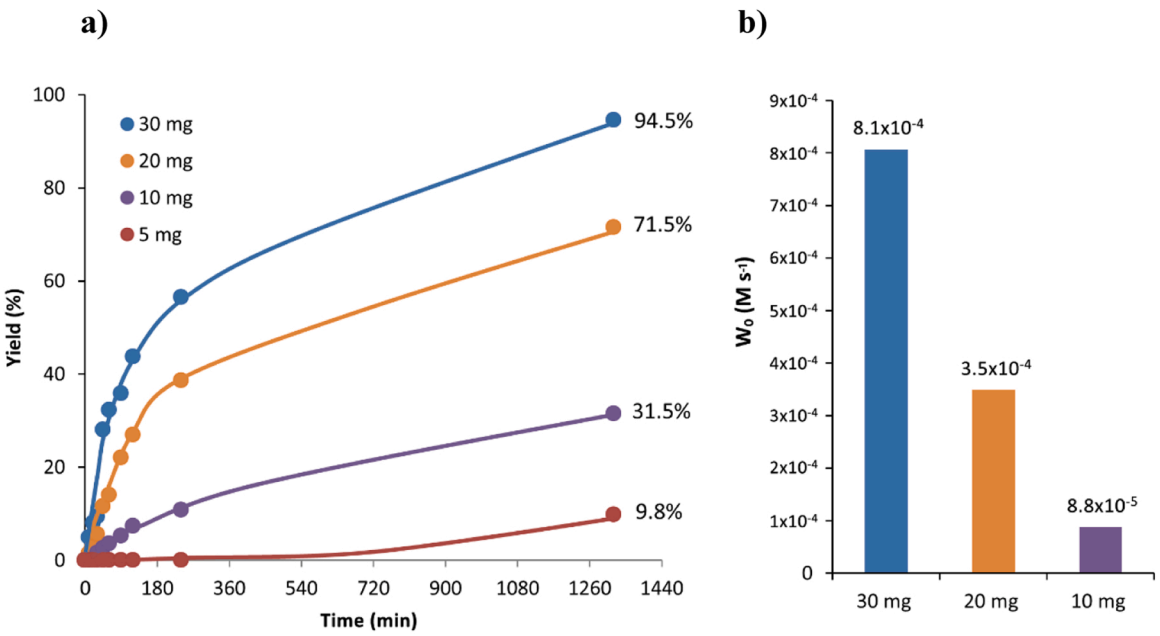

Fig. 7. The effect of MoCl@S13.5 loading on (a) the yield of diphenyl sulfide (%) with time and using $PhSiH_3$ as reductant, (b) the initial reaction rate ($W_0 = \Delta[s]/\Delta t$, M s^{-1}, s-diphenyl sulfide; Δt=60 min). Typical reaction conditions: diphenyl sulfoxide (0.25 mmol), $PhSiH_3$ (0.25 mmol), in 3 mL of acidified toluene (0.005 mM, HCl), 120 °C.

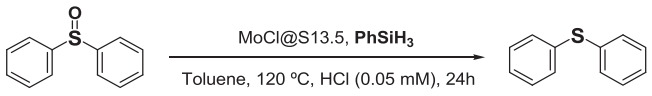

Scheme 2. Schematic representation of diphenyl sulfoxide reduction under the conditions reported in Fig. 8.

To better understand the role of the acid additive several assays were run using equal volumes of HCl solution with different concentrations, i.e., 5.0 mM or 0.005 mM (Scheme 3, Table S3). The results of these experiments (yield of sulfoxide and initial reaction rate) along with the assay without any acidified toluene are presented in Fig. 9. The highest initial reaction rate is observed at greater concentration of HCl (7.0×10^{-4} M s^{-1} for 5.0 mM - purple line - versus 3.5×10^{-4} M s^{-1} for 0.005 mM – yellow line). However, after 22 h of reaction time the yield of diphenyl sulfide is the same (81%) with or without the use of an acid promoter. In fact, regardless of the amount of $PhSiH_3$ used, higher HCl

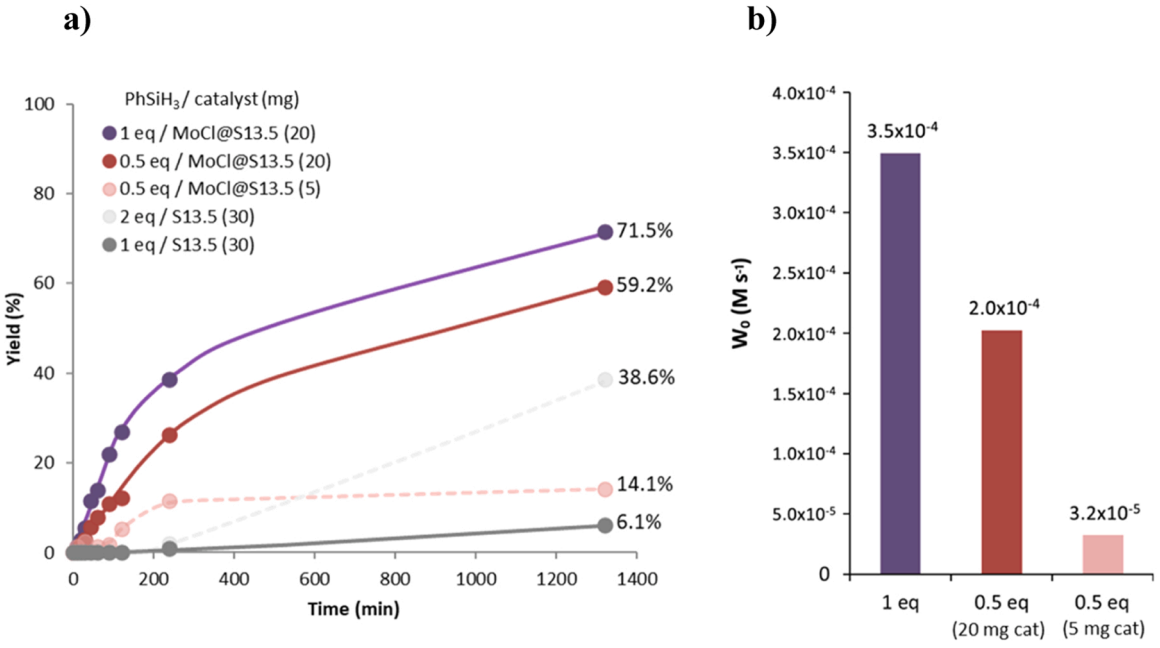

Fig. 8. Effect of the amount of reducing agent $PhSiH_3$ on (a) the yield of diphenyl sulfide in the presence of MoCl@S13.5 and S13.5 (acid-char), and (b) initial reaction rate of diphenyl sulfoxide reduction catalysed by MoCl@S13.5 ($W_0 = \Delta[s]/\Delta t$, M s^{-1}, s-diphenyl sulfide; Δt=60 min). Reaction conditions: diphenyl sulfoxide (0.25 mmol), catalyst (MoCl@S13.5: 5 or 20 mg, 8.0% Mo; S13.5: 30 mg), $PhSiH_3$ (0.125 mmol - 0.5 eq.; 0.25 mmol - 1 eq.; 0.5 mmol- 2 eq.), at 120 °C in acidified (0.005 mM, HCl) toluene (3 mL).

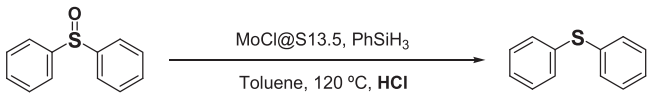

Scheme 3. Schematic representation of diphenyl sulfoxide reduction under the conditions reported in Fig. 9.

concentration results in the faster sulfoxide reduction, as reflected in higher initial reaction rate. Indeed, in the redox reaction $PhSiH_3 + Ph_2SO \rightarrow PhSi(OH)H_2 + Ph_2S$ mentioned above, the reduction of the sulfoxide requires an acidic medium. This accelerating effect of HCl has also been explained by the ability of Cl^- ions to act as ligands and stabilize MoCl or Mo-peroxo intermediates [43,60]. In fact, according to the literature, an increase of the concentration of HCl in a solution containing Mo(VI) complexes leads to the formation of chloro complexes in which the MoO_2^{2+} fragment is preserved throughout the acid concentration range [61]. On the other hand, previous studies have also highlighted a clear need of a slightly acidic medium [62,63] to achieve high yield of diphenyl sulfide [43].

The results reported in Fig. 9 also show the benefit of using the amounts of reducing agent lead to high initial reaction rates. Independently of the HCl amount used, assays where 0.250 mmol phenylsilane

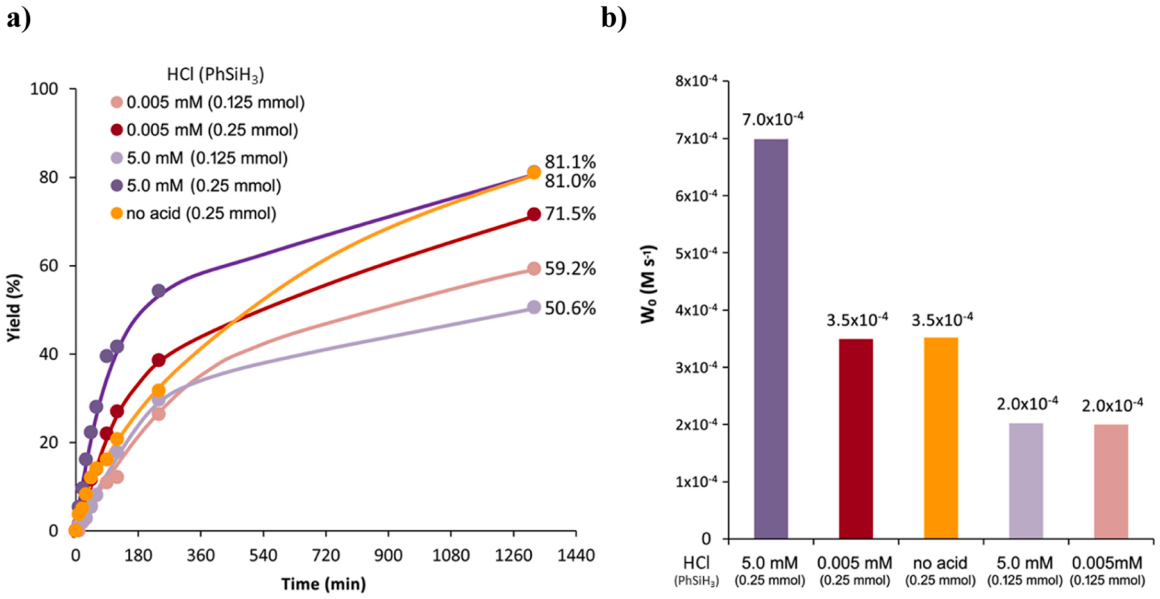

Fig. 9. The effect of HCl amount (a) on the yield of diphenyl sulfide in the reduction of diphenyl sulfoxide by $PhSiH_3$ catalysed by MoCl@S13.5 and (b) on initial reaction rate ($W_0 = \Delta[s]/\Delta t$, M s^{-1}, s-diphenyl sulfide; Δt=60 min). Reaction conditions: Sulfoxide (0.25 mmol), catalyst (20 mg, 8.0% Mo), $PhSiH_3$ (0.25 mmol or 0.25 mmol), in 3 mL of acidified toluene (0.005 mM or 5.0 mM of HCl), 120 °C.

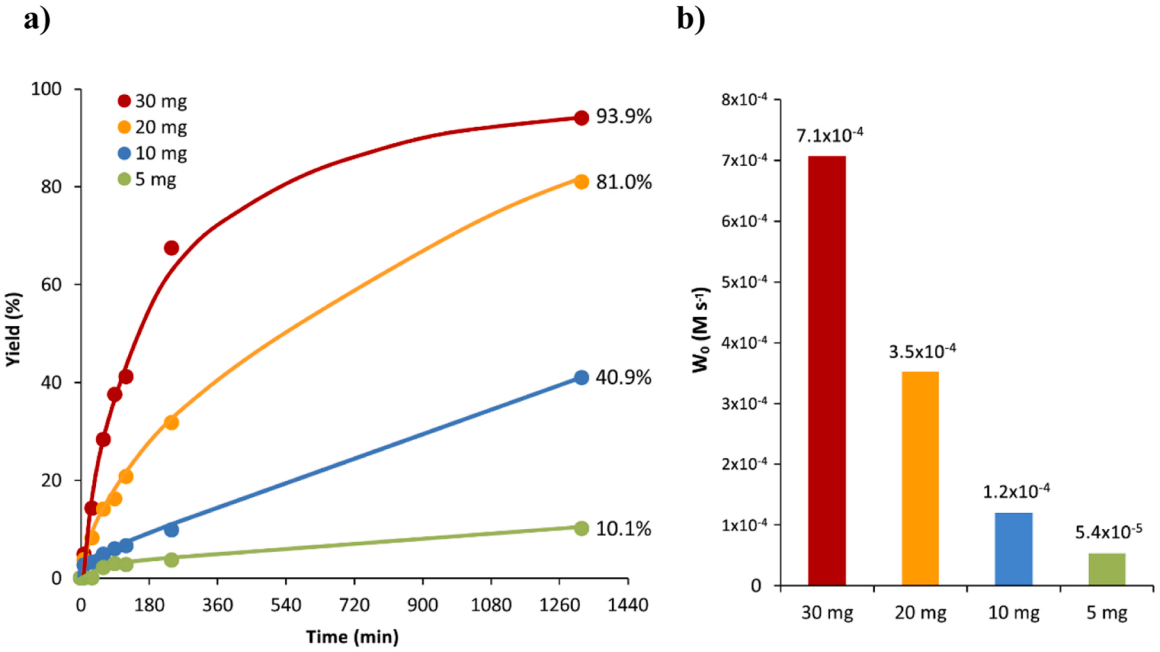

Fig. 10. The effect of catalyst amount (a) on the yield of diphenyl sulfide in the reduction of diphenyl sulfoxide by $PhSiH_3$ catalysed by MoCl@S13.5 and (b) on initial reaction rate ($W_0 = \Delta[s]/\Delta t$, M s^{-1}, s-diphenyl sulfide; Δt=60 min). Reaction conditions: Sulfoxide (0.25 mmol), catalyst (20 mg, 8.0% Mo), $PhSiH_3$ (0.25 mmol), in 3 mL of toluene without any acidification, 120 °C.

was used always presented higher W_0 values (e.g.: 7.0×10^{-4} M s^{-1} versus 3.5×10^{-4} M s^{-1} in the case of assays made with HCl 5.0 mM), than those obtained with 0.125 mmol of reducing agent. It is interesting to note that with the larger amount of phenylsilane and in the absence of acid promoter, initial reaction rates (W_0) reached the value of the assay in the presence of 0.005 M HCl. Considering this finding, a series of experiments was performed to evaluate the effect of different MoCl@S13.5 loadings in the absence of acid promoter (Table S4). The results (Fig. 10, Table S4) show that the diphenyl sulfide yield at different catalyst loading in the absence of HCl is comparable to that achieved in the presence of acid promoter (see Fig. 7). The initial rate values are also in the same order of magnitude with and without HCl, except when using 30 mg of MoCl@S13.5, when a faster reduction was observed in the absence of acid. It is important to emphasize that this set of data clearly shows the relevance of the acid-char support in the overall catalytic process, since it seems that the acidic surface groups of the acid-char support can perform the role of HCl. Due to these unexpected results we decided to also test the MoO@S13.5 for the deoxygenation of diphenyl sulfoxide into the equivalent sulfide in toluene without any acidification. The results obtained (see Table S5) show that when the quantity of $PhSiH_3$ was increased to 2 eq., an improvement in the yield of diphenyl sulfide was observed (37.8%).

The versatility of the MoCl@S13.5/$PhSiH_3$ system was tested in the reduction of another substrate, methyl phenyl sulfoxide, under the previously optimized reaction conditions (Scheme 4). As previously observed for diphenyl sulfoxide, the reduction of methyl phenyl sulfoxide does not occur in the absence of neither the MoCl@S13.5 catalyst nor the reducing agent (Table 3 entries 1 and 2). The blank assays with the acid-char show that, in the presence or in the absence of the HCl promoter, very low yields of methyl phenyl were obtained (6.1% and 8.6%, Table 3 entries 5 and 6, respectively). In the catalytic assays, a good yield of 83.1% was obtained after 24 h (using 10 mg of MoCl@S13.5 and HCl promoter, Table 3 entry 3), but even higher conversion (97.4%) was observed in absence of any acid promoter (Table 3, entry 4). The establishment of an acid-free protocol is potentially an extremely useful tool for organic synthesis, providing advantages in terms of sustainability and industrial application on a wide scale.

The successful deoxygenation of diphenyl and methyl phenyl sulfoxides suggested that the system MoCl@S13.5/phenylsilane might be efficient for the deoxygenation of additional sulfoxides (i.e., dibenzyl sulfoxide, dibutyl sulfoxide, and dimethyl sulfoxide). Excellent yields of the corresponding sulfides were obtained for all the sulfoxides under the optimized experimental conditions, in the absence of HCl (Table 4). In fact, apart from the dibenzyl sulfoxide, the maximum obtained yields of sulfides lie within 80% (diphenyl sulfide, Table 4 entry 1) - 97.4% (methyl phenyl sulfide, Table 4 entry 2). These data reveal the scope of the current catalytic system towards reduction of suitable substrates, such as diaryl, alkylaryl, dibenzyl, and dialkyl sulfoxide with a different degree of bulkiness and electronic properties. As in the case of dimethyl sulfoxide reduction, high conversions of other substituted sulfoxides were achieved in the absence of any acid promoter (Table 4).

3.3. Catalyst regeneration and reuse

The catalytic activity of MoCl@S13.5 used for the diphenyl sulfoxide reduction was evaluated for multiple use of catalyst under the conditions reported in Table S3 (see entries 9, 14 and 15). Thus, as an initial approach the catalyst was recovered from the reaction mixture by filtration and reused without any additional treatment. The diphenyl sulfide yield decreases from 81% to 19% (Table S3 entries 9 and 14) at equivalent catalyst loading. Taking into account the low direct reuse efficiency, a second approach of the catalyst regeneration was explored to determine whether the catalytic activity could be restored. After washing the used catalyst with dichloromethane (3 × 15 mL) and drying at 120 °C (1 h) the yield of diphenyl sulfide became 62.4 % in the second cycle (Table S3 entry 15).

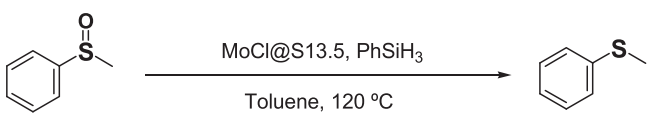

Scheme 4. .Schematic representation of methyl phenyl sulfoxide reduction under the conditions reported in Table 3.

Table 3
Methyl phenyl sulfoxide reduction to methyl phenyl sulfide using the MoCl@S13.5/phenylsilane catalytic system in toluene.[a].

Entry	Cat. (loading mg)	$PhSiH_3$ (equivalents to substrate)	HCl (mM)	Yield[b] [%]
1	–	1	0.005	<1
2	MoCl@S13.5 (10)	–	0.005	<1
3	MoCl@S13.5 (20)	1	0.005	83.1
4	MoCl@S13.5 (20)	1	–	97.4
5	S13.5 (30)	1	0.005	6.1
6	S13.5 (30)	1	–	8.6

[a] Reaction conditions: MoCl@S13.5 catalyst (20 mg), substrate (0.25 mmol), phenylsilane (0.25 mmol), toluene solvent (up to 3 mL total volume), 120 °C, 24 h.
[b] Yield of sulfide product [(moles of product/moles of substrate) × 100 %].

To study the possible leaching effect, 30 mg of MoCl@S13.5 catalyst was mixed with toluene and left under vigorous stirring for 1 h at 120 °C. After that, the catalyst was filtered out and diphenyl sulfoxide and phenylsilane were added to the remaining toluene solution and left to react for 24 h under standard reaction conditions. No conversion of diphenyl sulfoxide was observed, suggesting that there was no leaching of soluble active species, i.e., no release of molybdenum species from the solid support to the toluene solution. In fact, while after 2 h of reaction 100% yield was achieved using homogenous catalyst (entries 13 of Table 2 and S1) or a mixture of the acid-char and the homogenous catalyst (Table S1, entry 14). So, it can be concluded that no release of $[MoO_2Cl_2]$ into the reaction solution, from MoCl@S13.5, occurred.

To further evaluate possible leaching, the Mo amount of the catalyst recovered after the catalytic assay was determined by ICP-OES. The result (Table S6) demonstrates that no significant leaching of soluble Mo active species occurred as the difference from the amount determined in the fresh catalyst lies in the error range of the technique.

All the results previously discussed point out that some deactivation of the active centers of the immobilized catalyst may occur. This was demonstrated by the analysis of the FTIR spectrum of the material after the treatment with CH_2Cl_2 (see Fig. S5 and discussion in SI, page 9) that revealed the presence of organic compounds most liked adsorbed on the surface and/or interacting with the Mo centers.

In recent studies, it was possible to identify a comparable conversion of sulfoxides into sulfides using heterogeneous catalysts, but through a hydrogenation process [64–66]. High pressures (c.a. 10 atm) and the most variable temperature ranges are used in these operations [58,64]. Yao *et al.* used nitrogen-doped carbon-supported cobalt-molybdenum bimetallic catalysts, and Fujita *et al.* reported a titanium-dioxide-supported nickel phosphide nanoalloy (nano--Ni_2P/TiO_2) that exhibits high catalytic activity for the deoxygenation of various sulfoxides to sulfides under 1 bar of H_2 [63,64]. Mitsudome *et al.* illustrated the use of a continuous flow reactor with Ru nanoparticles supported on TiO_2 to enhance the selective hydrogenation of different functionalized sulfoxides at atmospheric H_2 pressure [58]. Kuwahara *et al.* demonstrated a far more complex system with the resource of plasmonic hydrogen molybdenum bronze coupled with Pt nanoparticles (Pt/H_xMoO_{3-y}) showing a high catalytic performance in the deoxygenation of sulfoxides with 1 atm of H_2 at room temperature, with activity

Table 4
Substrate scope in the reduction of sulfoxides to sulfides by the MoCl@S13.5/phenylsilane system in acid free toluene.[a].

Entry	Sulfoxide Substrate	Sulfide Product	Yield (%)[b]
1	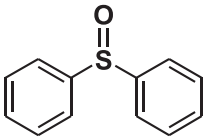	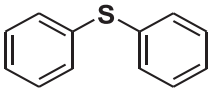	81.0
2	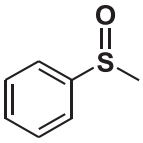	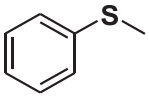	97.4
3	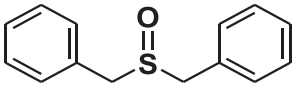	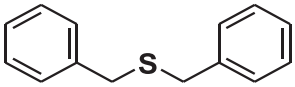	61.8[c]
4	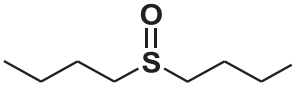	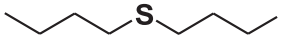	94.8
5			94.7

[a] Reaction conditions: MoCl@S13.5 catalyst (20 mg), substrate (0.25 mmol), phenylsilane (0.25 mmol), not acidified toluene (up to 3 mL total volume), 120 °C, 24 h.
[b] Yield of sulfide product [(moles of product/moles of substrate) × 100 %].
[c] Dibenzyl sulfone (34.7 %) is also formed as a by-product.

enhancement under visible light irradiation relative to dark conditions [65]. Sulfoxide deoxygenation processes have also been shown using hydroxyapatite-supported ruthenium nanoparticles as well as gold nanoparticles [67–69]. Nonetheless, the methodology used in the present study has the potential to be a significant instrument for organic synthesis, providing advantages in terms of sustainability. This is accomplished by the use of an economically accessible transition metal, a matrix from the valorization of industry wastes, and milder reaction conditions, which eliminate the need for acid promoters. Furthermore, the uniqueness of this work is not to report the use of an acid-biochar support for the first time, but to proof that it allows the preparation of a catalyst that can perform in very favorable conditions for the deoxygenation of sulfoxides. In fact, the capacity of the acid-char support to be the source of the acid required for the reduction was an added value for this particular reaction.

4. Conclusions

In this study we demonstrated the valorization of sisal rope industry wastes through the fabrication of an acid-char to be used as support for Mo-based catalysts, which were tested in the reduction of sulfoxides to sulfides. This carbon-based material prepared from biomass as a support, besides being environmentally sustainable, provided a good strategy to develop new heterogeneous catalysts. Molybdenum centers were immobilized on the surface of acid-char and tested as immobilized catalysts for sulfoxide deoxygenation, establishing the path for future heterogeneous catalysts based on industry by-product sustainability. The MoCl@S13.5 material acts as efficient catalyst in the heterogeneous reduction of diaryl, alkylaryl, dibenzyl, and dialkyl sulfoxides to the corresponding sulfides in the presence of phenylsilane.

The material MoCl@S13.5 manufactured from the acid-char as solid matrix has proved to be very useful, since the acidic character of its surface was an asset for sulfoxides reduction that usually requiresin the presence of an acid promoter or the addition of a catalyst in a solution with very low pH. The MoCl@S13.5 catalytic activity was promising since the heterogeneous catalyst could be reused following a simple regeneration process using dichloromethane. The same sulfoxide conversions occur substantially faster when employing the well-explored homogeneous [MoO_2Cl_2] catalyst, making it a viable choice for our research purpose; nevertheless, in those reported circumstances, the catalyst cannot be easily isolated for equivalent Mo catalyst loadings. The effort required to reuse and separate transition metals is highly valued, not only for its economic worth but also for its availability. The approach herein described may also be applied to more precious metals that have affinity for the functional groups on the surface of acid-chars. This reuse enables the extension of Mo-based catalysts to new applications, contributing to the development of more sustainable and economically viable industrial processes, lowering costs and environmental impact, and opening up new pathways for the development of sustainable products.

Synopsis

Valorization of wastes from the sisal rope industry by preparing and converting acid-chars into immobilized molybdenum catalysts: full characterization and use as heterogeneous catalysts for the reduction of sulfoxides to sulfides.

CRediT authorship contribution statement

Tiago A. Fernandes: Conceptualization, Data curation, Investigation, Methodology, Visualization, Writing – original draft, Writing – review & editing. **Tiago A.G. Duarte:** Investigation. **Ana S. Mestre:** Investigation, Methodology, Writing - original draft, Writing - review & editing. **Maria J.G. Ferreira:** Investigation, Visualization Writing – original draft. **Ana M. Botelho do Rego:** Investigation, Visualization Writing – original draft. **Ana M. Ferraria:** Investigation, Methodology. **Marina V. Kirillova:** Methodology, Writing – review & editing. **Ana P. Carvalho:** Conceptualization, Data curation, Funding acquisition, Investigation, Methodology, Supervision, Writing – original draft, Writing – review & editing. **Maria José Calhorda:** Data curation, Funding acquisition, Supervision, Writing – review & editing.

Declaration of Competing Interest

The authors declare the following financial interests/personal

relationships which may be considered as potential competing interests: Ana P. Carvalho reports financial support was provided by Fundação para a Ciência e a Tecnologia. Ana S. Mestre reports was provided by Fundação para a Ciência e Tecnologia. Tiago Fernandes reports was provided by Fundação para a Ciência e a Tecnologia. Nothing to declare.

Data availability

Data will be made available on request.

Acknowledgements

This work was supported by Fundação para a Ciência e a Tecnologia (FCT) through projects PEst-OE/FIS/UI0261/2014, PEst-OE/MULTI/UI0612/2013, UIDB/04046/2020 and UIDP/04046/2020 (BioISI), UIDB/00100/2020 and UIDP/00100/2020 (CQE), Lisboa-01–2020, LA/P/0056/2020 (IMS), UIDB/04565/2020, UIDP/04565/2020 (iBB), LA/P/0140/2020 (i4HB) and 0145FEDER-022125-IST/RNEM. TAF thanks CQB and FCT for a fellowship (PEst-OE/MULTI/00612/2013) and CEECIND/02725/2018 contract. ASM thanks FCT for the CEECIND/01371/2017 contract (Embrace Project). AMF thanks FCT and IST, Portugal, for contract no. IST-ID/131/2018. The authors thank Isabel Dias Nogueira for acquisition and refinement of SEM images. We thank Eng. Mário Dias (LAIST) for ICP-OES experimental assistance.

Appendix A. Supporting information

Supporting Information is available and contains: Experimental procedures to determine the $pH_{PZC,}$ apparent density and moisture content of the acid-char, synthesis for the diethyl ether solution of $[MoO_2Cl_2(H_2O)_2]$, GC chromatographic evolution of diphenyl sulfoxide reduction catalyzed by MoCl@S13.5 (Fig. S1), SEM-EDS analysis of MoO@S13.5 with spectrum of selected area (Fig. S2), solid state NMR – CP/MAS and continuous-wave (CW) decoupling of MoO@S13.5, MoCl@S13.5 and S13.5 (Figs. S3 and S4), additional catalytic results (Tables S1−S5), Mo content analysis performed by ICP-OES (Table S6), and FTIR analysis of MoCl@S13.5 before and after catalysis (Fig. S5). Supplementary data associated with this article can be found in the online version at doi:10.1016/j.cattod.2023.114388.

References

[1] Q.H. Xia, H.Q. Ge, C.P. Ye, Z.M. Liu, K.X. Su, Advances in homogeneous and heterogeneous catalytic asymmetric epoxidation, Chem. Rev. 105 (2005) 1603–1662, https://doi.org/10.1021/cr0406458.
[2] J.C. Bailar, “Heterogenizing” homogeneous catalysts, Catal. Rev. 10 (1974) 17–36, https://doi.org/10.1080/01614947408079625.
[3] J.L.F. Philippe Serp, Carbon Materials for Catalysis, Wiley InterScience, John Wiley & Sons, Inc,, New Jersey, 2009.
[4] A. Martins, N. Nunes, A.P. Carvalho, L.M.D.R.S. Martins, Zeolites and related materials as catalyst supports for hydrocarbon oxidation reactions, Catalysts 12 (2022) 154, https://doi.org/10.3390/catal12020154.
[5] C.I.M. Santos, G. Gonçalves, M. Cicuéndez, I. Mariz, V.S. Silva, H. Oliveira, F. Campos, S.I. Vieira, P.A.A.P. Marques, E.M.S. Maçôas, M.G.P.M.S. Neves, J.M. G. Martinho, Biocompatible hybrids based on nanographene oxide covalently linked to glycolporphyrins: synthesis, characterization and biological evaluation, Carbon 135 (2018) 202–214, https://doi.org/10.1016/j.carbon.2018.04.040.
[6] C.I.M. Santos, L. Rodríguez-Pérez, G. Gonçalves, S.N. Pinto, M. Melle-Franco, P.A. A.P. Marques, M.A.F. Faustino, M.Á. Herranz, N. Martin, M.G.P.M.S. Neves, J.M. G. Martinho, E.M.S. Maçôas, Novel hybrids based on graphene quantum dots covalently linked to glycol corroles for multiphoton bioimaging, Carbon 166 (2020) 164–174, https://doi.org/10.1016/j.carbon.2020.04.012.
[7] T.W. van Deelen, H. Yoshida, R. Oord, J. Zečević, B.M. Weckhuysen, K.P. de Jong, Cobalt nanocrystals on carbon nanotubes in the Fischer-Tropsch synthesis: impact of support oxidation, Appl. Catal. A Gen. 593 (2020), 117441, https://doi.org/10.1016/j.apcata.2020.117441.
[8] M. Sutradhar, L.M.D.R.S. Martins, S.A.C. Carabineiro, M.F.C. Guedes da Silva, J. G. Buijnsters, J.L. Figueiredo, A.J.L. Pombeiro, Oxidovanadium(V) complexes anchored on carbon materials as catalysts for the oxidation of 1-phenylethanol, ChemCatChem 8 (2016) 2254–2266, https://doi.org/10.1002/cctc.201600316.
[9] H. Gaspar, M. Andrade, C. Pereira, A.M. Pereira, S.L.H. Rebelo, J.P. Araújo, J. Pires, A.P. Carvalho, C. Freire, Alkene epoxidation by manganese(III) complexes immobilized onto nanostructured carbon CMK-3, Catal. Today (2013) 103–110, https://doi.org/10.1016/j.cattod.2012.04.018.
[10] M.J. Prauchner, S.C. Oliveira, F. Rodríguez-Reinoso, Tailoring low-cost granular activated carbons intended for CO_2 adsorption, Front. Chem. 8 (2020), 581133, https://doi.org/10.3389/fchem.2020.581133.
[11] M.A. Andrade, A.S. Mestre, A.P. Carvalho, A.J.L. Pombeiro, L.M.D.R.S. Martins, The role of nanoporous carbon materials in catalytic cyclohexane oxidation, Catal. Today 357 (2020) 46–55, https://doi.org/10.1016/j.cattod.2019.07.036.
[12] A.S. Mestre, A.P. Carvalho, Nanoporous carbon synthesis: an old story with exciting new chapters, in: T.H. Ghrib (Ed.), Porosity - Process, Technologies and Applications, InTechOpen, 2018, https://doi.org/10.5772/intechopen.72476.
[13] Z. Ahmad, B. Gao, A. Mosa, H. Yu, X. Yin, A. Bashir, H. Ghoveisi, S. Wang, Removal of Cu(II), Cd(II) and Pb(II) ions from aqueous solutions by biochars derived from potassium-rich biomass, J. Clean. Prod. 180 (2018) 437–449, https://doi.org/10.1016/j.jclepro.2018.01.133.
[14] D. Mohan, C.U. Pittman, M. Bricka, F. Smith, B. Yancey, J. Mohammad, P.H. Steele, M.F. Alexandre-Franco, V. Gómez-Serrano, H. Gong, Sorption of arsenic, cadmium, and lead by chars produced from fast pyrolysis of wood and bark during bio-oil production, J. Colloid Interface Sci. 310 (2007) 57–73, https://doi.org/10.1016/j.jcis.2007.01.020.
[15] J. Fang, L. Zhan, Y.S. Ok, B. Gao, Minireview of potential applications of hydrochar derived from hydrothermal carbonization of biomass, J. Ind. Eng. Chem. 57 (2018) 15–21, https://doi.org/10.1016/j.jiec.2017.08.026.
[16] T.S. Hubetska, A.S. Mestre, N.G. Kobylinska, A.P. Carvalho, Steam activation of acid-Chars for enhanced textural properties and pharmaceuticals removal, Nanomaterials 12 (2022) 3480, https://doi.org/10.3390/nano12193480.
[17] A.S. Mestre, F. Hesse, C. Freire, C.O. Ania, A.P. Carvalho, Chemically activated high grade nanoporous carbons from low density renewable biomass (Agave sisalana) for the removal of pharmaceuticals, J. Colloid Interface Sci. 536 (2019) 681–693, https://doi.org/10.1016/j.jcis.2018.10.081.
[18] L. Wang, Y. Guo, Y. Zhu, Y. Li, Y. Qu, C. Rong, X. Ma, Z. Wang, A new route for preparation of hydrochars from rice husk, Bioresour. Technol. 101 (2010) 9807–9810, https://doi.org/10.1016/j.biortech.2010.07.031.
[19] L. Wang, Y. Guo, B. Zou, C. Rong, X. Ma, Y. Qu, Y. Li, Z. Wang, High surface area porous carbons prepared from hydrochars by phosphoric acid activation, Bioresour. Technol. 102 (2011) 1947–1950, https://doi.org/10.1016/j.biortech.2010.08.100.
[20] A.P. Carvalho, A.S. Mestre, Acid-chars - versatile materials for adsorption and catalysis, Boletin Del. Grupo Esp. Del. Carbon 54 (2019) 33–38.
[21] Y. Cui, J.D. Atkinson, Tailored activated carbon from glycerol: role of acid dehydrator on physiochemical characteristics and adsorption performance, J. Mater. Chem. A 5 (2017) 16812–16821, https://doi.org/10.1039/C7TA02898A.
[22] Q. Ge, Q. Tian, M. Moeen, S. Wang, Facile synthesis of cauliflower leaves biochar at low temperature in the air atmosphere for Cu(II) and Pb(II) removal from water, Materials 13 (2020) 3163, https://doi.org/10.3390/ma13143163.
[23] C. Petit, M.V. Silva, A.S. Mestre, C.O. Ania, P.D. Vaz, A.P. Carvalho, C.D. Nunes, Solventless olefin epoxidation using a Mo–loaded sisal derived acid-char catalyst, ChemistrySelect 3 (2018) 10357–10363, https://doi.org/10.1002/slct.201802055.
[24] Y. Li, Y.-W. Mai, L. Ye, Sisal fibre and its composites: a review of recent developments, Compos. Sci. Technol. 60 (2000) 2037–2055, https://doi.org/10.1016/S0266-3538(00)00101-9.
[25] M. Saxena, A. Pappu, R. Haque, A. Sharma, Sisal fiber-based polymer composites and their applications, in: S. Kalia, B.S. Kaith, I. Kaur (Eds.), Cellulose Fibers: Bio- and Nano-Polymer Composites, Springer, Berlin, Heidelberg, 2011, pp. 589–659, https://doi.org/10.1007/978-3-642-17370-7_22.
[26] FAOSTAT, Food and Agricultural Commodities Production / Countries by Commodity (2020). ⟨http://Www.Fao.Org/Faostat/En/#data⟩.
[27] M. Andrade, J.B. Parra, M. Haro, A.S. Mestre, A.P. Carvalho, C.O. Ania, Characterization of the different fractions obtained from the pyrolysis of rope industry waste, J. Anal. Appl. Pyrolysis 95 (2012) 31–37, https://doi.org/10.1016/j.jaap.2012.01.002.
[28] R. Hille, J. Rétey, U. Bartlewski-Hof, W. Reichenbecher, B. Schink, Mechanistic aspects of molybdenum-containing enzymes, FEMS Microbiol. Rev. 22 (1998) 489–501, https://doi.org/10.1111/j.1574-6976.1998.tb00383.x.
[29] R. Hille, The Mononuclear molybdenum enzymes, Chem. Rev. 96 (1996) 2757–2816, https://doi.org/10.1021/cr950061t.
[30] C. Chatgilialoglu, K.-D.A. Asmus, NATO Advanced Study Institute on Sulfur-Centered Reactive Intermediates in Chemistry and Biology (Eds.), Sulfur-centered Reactive Intermediates in Chemistry and Biology, Plenum Press, New York, 1990.
[31] T.A. Fernandes, A.C. Fernandes, Dioxomolybdenum complexes as excellent catalysts for the deoxygenation of aryl ketones to aryl alkenes, ChemCatChem 7 (2015) 3503–3507, https://doi.org/10.1002/cctc.201500560.
[32] E. Armakola, I.R. Salcedo, M. Bazaga-García, P. Olivera-Pastor, G. Mezei, A. Cabeza, T.A. Fernandes, A.M. Kirillov, K.D. Demadis, Phosphonate decomposition-induced polyoxomolybdate Dumbbell-type cluster formation: structural analysis, proton conduction, and catalytic sulfoxide reduction, Inorg. Chem. 58 (2019) 11522–11533, https://doi.org/10.1021/acs.inorgchem.9b01376.
[33] S.C.A. Sousa, T.A. Fernandes, A.C. Fernandes, Highly efficient deoxygenation of aryl ketones to arylalkanes catalyzed by dioxidomolybdenum complexes, Eur. J. Org. Chem. 18 (2016) 3109–3112, https://doi.org/10.1002/ejoc.201600441.
[34] P.M. Reis, P.J. Costa, C.C. Romão, J.A. Fernandes, M.J. Calhorda, B. Royo, Hydrogen activation by high-valent oxo-molybdenum(vi) and -rhenium(vii) and -(v) compounds, Dalton Trans. (2008) 1727–1733, https://doi.org/10.1039/b719375k.

[35] A.C. Fernandes, C.C. Romão, A novel method for the reduction of sulfoxides and pyridine N-oxides with the system silane/MoO_2Cl_2, Tetrahedron 62 (2006) 9650–9654, https://doi.org/10.1016/j.tet.2006.07.077.

[36] A.C. Fernandes, C.C. Romão, Reduction of sulfoxides with boranes catalyzed by MoO_2Cl_2, Tetrahedron Lett. 48 (2007) 9176–9179, https://doi.org/10.1016/j.tetlet.2007.10.106.

[37] F.J. Arnáiz, R. Aguado, M.R. Pedrosa, A. De Cian, Addition compounds of dichlorodioxomolybdenum(VI) with sulfoxides. Molecular structure of $[MoO_2Cl_2(Me_2SO)_2]$, Inorg. Chim. Acta 347 (2003) 33–40, https://doi.org/10.1016/S0020-1693(02)01434-2.

[38] W.T. Dixon, J. Schaefer, M.D. Sefcik, E.O. Stejskal, R.A. McKay, Total suppression of sidebands in CPMAS C-13 NMR, J. Magn. Reson. (1969) 49 (1982) 341–345, https://doi.org/10.1016/0022-2364(82)90199-8.

[39] A.P. Carapeto, A.M. Ferraria, A.M.B. do Rego, Unravelling the reaction mechanism of silver ions reduction by chitosan from so far neglected spectroscopic features, Carbohydr. Polym. 174 (2017) 601–609, https://doi.org/10.1016/j.carbpol.2017.06.100.

[40] J.S. Noh, J.A. Schwarz, Estimation of the point of zero charge of simple oxides by mass titration, J. Colloid Interface Sci. 130 (1989) 157–164, https://doi.org/10.1016/0021-9797(89)90086-6.

[41] A.S. Mestre, J. Pires, J.M.F. Nogueira, A.P. Carvalho, Activated carbons for the adsorption of ibuprofen, Carbon 45 (2007) 1979–1988, https://doi.org/10.1016/j.carbon.2007.06.005.

[42] Y. Wang, D. Wang, M. Tan, B. Jiang, J. Zheng, N. Tsubaki, M. Wu, Monodispersed hollow SO_3H-functionalized carbon/silica as efficient solid acid catalyst for esterification of oleic acid, ACS Appl. Mater. Interfaces 7 (2015) 26767–26775, https://doi.org/10.1021/acsami.5b08797.

[43] B. Zhang, J. Ren, X. Liu, Y. Guo, Y. Guo, G. Lu, Y. Wang, Novel sulfonated carbonaceous materials from p-toluenesulfonic acid/glucose as a high-performance solid-acid catalyst, Catal. Commun. 11 (2010) 629–632, https://doi.org/10.1016/j.catcom.2010.01.010.

[44] S. Kang, J. Ye, Y. Zhang, J. Chang, Preparation of biomass hydrochar derived sulfonated catalysts and their catalytic effects for 5-hydroxymethylfurfural production, RSC Adv. 3 (2013) 7360–7366, https://doi.org/10.1039/C3RA23314F.

[45] J.M. Coddington, M.J. Taylor, Molybdenum-95 nuclear magnetic resonance and vibrational spectroscopic studies of molybdenum(VI) species in aqueous solutions and solvent extracts from hydrochloric and hydrobromic acid: evidence for the complexes $[Mo_2O_5(H_2O)_6]^{2+}$, $[MoO_2X_2(H_2O)_2]$(X = Cl or Br), and $[MoO_2Cl_4]^{2-}$, J. Chem. Soc., Dalton Trans. (1990) 41–47, https://doi.org/10.1039/DT9900000041.

[46] F.A. Schröder, R. Mattes, Vibrational spectra of $MoO_3{\cdot}2H_2O$ and $MoO_2Cl_2{\cdot}H_2O$, Z. Nat. 27 (1972) 22–25, https://doi.org/10.1515/znb-1972-0105.

[47] S. Biniak, G. Szymanski, J. Siedlewski, A. Swiatkowski, The characterization of activated carbons with oxygen and nitrogen surface groups, Carbon 35 (1997) 1799–1810, https://doi.org/10.1016/S0008-6223(97)00096-1.

[48] P.E. Fanning, M.A. Vannice, A DRIFTS study of the formation of surface groups on carbon by oxidation, Carbon 31 (1993) 721–730, https://doi.org/10.1205/026387603765444537.

[49] C.E. Brewer, K. Schmidt-Rohr, J.A. Satrio, R.C. Brown, Characterization of biochar from fast pyrolysis and gasification systems, Environ. Prog. Sustain. Energy 28 (2009) 386–396, https://doi.org/10.1002/ep.10378.

[50] D.C. Apperley, R.K. Harris, P. Hodgkinson, Solid State NMR: Basic Principles & Practice, Momentum Press, New York, 2012.

[51] J. Światowska-Mrowiecka, S. de Diesbach, V. Maurice, S. Zanna, L. Klein, E. Briand, I. Vickridge, P. Marcus, Li-ion intercalation in thermal oxide thin films of MoO_3 as studied by XPS, RBS, and NRA, J. Phys. Chem. C 112 (2008) 11050–11058, https://doi.org/10.1021/jp800147f.

[52] A.V. Naumkin, A. Kraut-Vass, S.W. Gaarenstroom, C.J. Powell, NIST X-ray Photoelectron Spectroscopy Database. NIST Standard Reference Database 20, Version 4.1., ⟨https://srdata.nist.gov/xps/Default.aspx⟩. (Accessed 19 January 2023).

[53] L.E. Pimentel Real, A.M. Ferraria, A.M. Botelho do Rego, Comparison of different photo-oxidation conditions of poly(vinyl chloride) for outdoor applications, Polym. Test. 27 (2008) 743–751, https://doi.org/10.1016/j.polymertesting.2008.05.009.

[54] G. Beamson, D. Briggs, High resolution XPS of organic polymers. The Scienta ESCA300 Database, Wiley, Chichester, 1992.

[55] E. Pellegrin, V. Perez-Dieste, C. Escudero, P. Rejmak, N. Gonzalez, A. Fontsere, J. Prat, J. Fraxedas, S. Ferrer, Water/methanol solutions characterized by liquid μ-jet XPS and DFT—the methanol hydration case, J. Mol. Liq. 300 (2020), 112258, https://doi.org/10.1016/j.molliq.2019.112258.

[56] A.I. Melato, L.M. Abrantes, A.M. Botelho do Rego, $Fe(CN)_6^{3-}$ incorporation on Poly (3,4-ethylenedioxythiophene) films: preparation and X-ray Photoelectron Spectroscopy characterization of the modified electrodes, Thin Solid Films 518 (2010) 1947–1952, https://doi.org/10.1016/j.tsf.2009.07.157.

[57] E.C.B.A. Alegria, E. Fontolan, A.P.C. Ribeiro, M.N. Kopylovich, C. Domingos, A. M. Ferraria, R. Bertani, A.M. Botelho do Rego, A.J.L. Pombeiro, Simple solvent-free preparation of dispersed composites and their application as catalysts in oxidation and hydrocarboxylation of cyclohexane, Mater. Today Chem. 5 (2017) 52–62, https://doi.org/10.1016/j.mtchem.2017.07.002.

[58] T. Mitsudome, Y. Takahashi, T. Mizugaki, K. Jitsukawa, K. Kaneda, Hydrogenation of sulfoxides to sulfides under mild conditions using ruthenium nanoparticle catalysts, Angew. Chem. Int. Ed. 53 (2014) 8348–8351, https://doi.org/10.1002/anie.201403425.

[59] X. Sun, D. Haas, K. Sayre, D. Weller, Formation of diphenyl sulfoxide and diphenyl sulfide via the aluminum chloride–facilitated electrophilic aromatic substitution of benzene with thionyl chloride, and a novel reduction of sulfur (IV) to sulfur (II), Phosphorus Sulfur Silicon Relat. Elem. 185 (2010) 2535–2542, https://doi.org/10.1080/10426501003733849.

[60] F.P. Byrne, S. Jin, G. Paggiola, T.H.M. Petchey, J.H. Clark, T.J. Farmer, A.J. Hunt, C. Robert McElroy, J. Sherwood, Tools and techniques for solvent selection: green solvent selection guides, Sustain. Chem. Process. 4 (2016) 7, https://doi.org/10.1186/s40508-016-0051-z.

[61] P. Tkac, A. Paulenova, Speciation of molybdenum(VI) in aqueous and organic phases of selected extraction systems, Sep. Sci. Technol. 43 (2008) 2641–2657, https://doi.org/10.1080/01496390802122261.

[62] M.V. Kirillova, T.A. Fernandes, V. André, A.M. Kirillov, Mild C–H functionalization of alkanes catalyzed by bioinspired copper (II) cores, Org. Biomol. Chem. 17 (2019) 7706–7714, https://doi.org/10.1039/C9OB01442J.

[63] T.A. Fernandes, C.I.M. Santos, V. André, S.S.P. Dias, M.V. Kirillova, A.M. Kirillov, New aqua-soluble dicopper(II) aminoalcoholate cores for mild and water-assisted catalytic oxidation of alkanes, Catal. Sci. Technol. 6 (2016) 4584–4593, https://doi.org/10.1039/C5CY02084K.

[64] K. Yao, Z. Yuan, S. Jin, Q. Chi, B. Liu, R. Huang, Z. Zhang, Efficient hydrodeoxygenation of sulfoxides into sulfides under mild conditions using heterogeneous cobalt–molybdenum catalysts, Green Chem. 22 (2020) 39–43, https://doi.org/10.1039/C9GC02465D.

[65] S. Fujita, S. Yamaguchi, S. Yamazoe, J. Yamasaki, T. Mizugaki, T. Mitsudome, Nickel phosphide nanoalloy catalyst for the selective deoxygenation of sulfoxides to sulfides under ambient H_2 pressure, Org. Biomol. Chem. 18 (2020) 8827–8833, https://doi.org/10.1039/d0ob01603a.

[66] Y. Kuwahara, Y. Yoshimura, K. Haematsu, H. Yamashita, Mild deoxygenation of sulfoxides over plasmonic molybdenum oxide hybrid with dramatic activity enhancement under visible light, J. Am. Chem. Soc. 140 (2018) 9203–9210, https://doi.org/10.1021/jacs.8b04711.

[67] Y. Takahashi, T. Mitsudome, T. Mizugaki, K. Jitsukawa, K. Kaneda, Highly efficient deoxygenation of sulfoxides using hydroxyapatite-supported ruthenium nanoparticles, Chem. Lett. 43 (2014) 420–422, https://doi.org/10.1246/cl.131077.

[68] Y. Mikami, A. Noujima, T. Mitsudome, T. Mizugaki, K. Jitsukawa, K. Kaneda, Highly efficient gold nanoparticle catalyzed deoxygenation of amides, sulfoxides, and pyridine N-oxides, Chem. Eur. J. 17 (2011) 1768–1772, https://doi.org/10.1002/chem.201003109.

[69] T. Mitsudome, K. Kaneda, Gold nanoparticle catalysts for selective hydrogenations, Green Chem. 15 (2013) 2636–2654, https://doi.org/10.1039/C3GC41360H.